

“Synthesis, cell-surface binding and cellular uptake of fluorescently labelled glucose-DNA conjugates with different carbohydrate presentation” Ugarte-Urbe, B., Pérez-Rentero, S., Lucas, R., Aviñó, A., Reina, J.J., Alkorta, I., Eritja, R., Morales, J.C. *Bioconjugate Chem.*, 21(7), 1280-1287 (2010). doi: 10.1021/bc100079n

Synthesis, cell-surface binding and cellular uptake of fluorescently labelled glucose-DNA conjugates with different carbohydrate presentation

*Begoña Ugarte-Urbe,[§] Sonia Pérez-Rentero,[‡] Ricardo Lucas,[†] Anna Aviñó,[‡] José J. Reina,[†]
Itziar Alkorta,[§] Ramón Eritja,[‡] Juan C. Morales^{*,†}*

[§] Unidad de Biofísica, Centro Mixto CSIC-UPV/EHU, Universidad del País Vasco, 48080 Bilbao, Spain.

[‡] Institute for Research in Biomedicine (IRB Barcelona), Institute for Advanced Chemistry of Catalonia (IQAC-CSIC), Networking Centre on Bioengineering, Biomaterials and Nanomedicine (CIBER-BBN), Edifici Helix, Baldiri Reixac 15, E-08028 Barcelona, Spain.

[†] Instituto de Investigaciones Químicas, CSIC – Universidad de Sevilla, 49 Americo Vesputio, 41092 Sevilla, Spain.

AUTHOR EMAIL ADDRESS: jcmorales@iiq.csic.es

TITLE RUNNING HEAD. Cellular uptake of glucose DNA conjugates.

ABSTRACT

Oligonucleotide conjugates carrying carbohydrates at the 5'-end have been prepared. Glucose, fucose and saccharides containing glucose at the non-reducing end were attached to DNA strands using the classical phosphoramidite chemistry. Two types of spacers and a dendron scaffold helped to obtain a diversity of sugar presentations in the DNA conjugates. Cellular surface adsorption and cellular uptake of carbohydrate oligonucleotide antisense sequences were measured using flow cytometric analysis. Conjugates with the glucose moiety linked through long spacers (15 to 18 atom distances) were better internalized than those with short linkers (4 atom distance) and than DNA control strands without sugar modification. Conjugates with tetravalent presentation of glucose did not improve cell uptake.

KEYWORDS carbohydrate oligonucleotide conjugates, DNA, cellular uptake, cell-surface adsorption, multivalency, oligonucleotide synthesis.

INTRODUCTION

In the last two decades new compounds based on the use of small synthetic nucleic acids have shown promising results as potential drugs (*1, 2*). Oligonucleotides have been used for the inhibition of a specific gene by blocking gene translation or gene transcription or by stimulating the degradation of a particular messenger RNA. Several strategies have been developed for this purpose. In the antisense strategy, synthetic oligonucleotides complementary to the messenger RNA of a given gene have been used to inhibit translation of messenger RNA to protein (*3, 4*). In the antigene strategy, triplex-forming oligonucleotides may interact with double-stranded DNA inhibiting DNA transcription (*5-7*). More recently, in the siRNA strategy, small RNA duplexes complementary to messenger RNA sequences bind a protein complex named RISC. The complex formed by the antisense or guide RNA strand and RISC is able to catalyze the efficient degradation of a specific messenger RNA, lowering the amount of target protein (*8-10*).

Among the problems found during the development of oligonucleotides as drugs are their degradation by exonucleases under physiological conditions, and particularly their low cell uptake due to their highly polar character and large size. Most of the improvements in the design of nucleic acid derivatives have been directed to enhance stability against nucleases and/or to improve cellular uptake without hindering the hybridisation properties that are vital for the efficient gene inhibitory properties of the oligonucleotides. Conjugation of siRNA to different delivery carriers such as lipids (*11*), polymers (*12, 13*) or peptides (*14*) has been reported for improved delivery of siRNA. Moreover, cationic carriers are among the most efficient strategies for cell uptake although many of them exhibit severe cytotoxicity (*15*). At the same time, covalent conjugation of oligonucleotides to peptides or to hydrophobic moieties has been used to facilitate internalization (*16, 17*). For example, cholesterol-DNA and siRNA conjugates have shown improved inhibitory properties (*18-20*).

A possible alternative to enhance oligonucleotide uptake is the preparation of carbohydrate oligonucleotide conjugates (COCs) that may use sugar binding membrane receptors to mediate cell entry. Different COCs have been synthesized up to date (*16, 21, 22*) but only a few have been

experimentally tested. Recently, antisense oligonucleotides conjugated to multivalent hyaluronan disaccharide did not show higher or more specific uptake than unconjugated oligonucleotides in a cell line expressing the hyaluronan receptor CD44 (23). In contrast, Mahato et al. has utilized mannose 6-phosphate-bovine serum albumin and galactose polyethyleneglycol conjugated to oligonucleotides for site-specific delivery into hepatic cells when injected to rats (24, 25). Also, siRNA carrying lactose linked through a polyethylene glycol branch at the 5'-end of the sense strand immersed in a polyionic complex micelle has been shown to enhance gene silencing in hepatoma cells (26).

Glucose is essential for cell survival and its transport is facilitated by members of the GLUT protein family. We reasoned that oligonucleotide conjugates carrying glucose moieties could bind to GLUT receptors and facilitate internalization via receptor-mediated endocytosis. In the present work we have prepared oligonucleotides modified at the 5'-end with glucose or glucose-containing saccharides at the non-reducing end (Figure 1). Two types of spacers and a dendron scaffold have been used to probe a diversity of sugar presentations. A carbohydrate-oligonucleotide conjugate containing a fucose unit was also prepared as a negative control. We have covalently bound the carbohydrate moieties to a single-stranded oligodeoxynucleotide antisense sequence and finally added a fluorescence tag. The corresponding labeled carbohydrate-oligonucleotide conjugates have been used to study their cell-surface binding and their cellular uptake in HeLa and U87.CD4.CXCR4 cell lines using flow cytometric analysis.

EXPERIMENTAL PROCEDURES

General methods and materials. All chemicals were obtained from chemical suppliers and used without further purification, unless otherwise noted. All reactions were monitored by TLC on precoated Silica-Gel 60 plates F254, and detected by heating with Mostain (500 ml of 10% H_2SO_4 , 25g of $(\text{NH}_4)_6\text{Mo}_7\text{O}_{24}\cdot 4\text{H}_2\text{O}$, 1g $\text{Ce}(\text{SO}_4)_2\cdot 4\text{H}_2\text{O}$). Products were purified by flash chromatography with silica gel 60 (200-400 mesh). NMR spectra were recorded on either a Bruker AVANCE 300 or ARX 400 MHz [300 or 400 MHz (^1H), 75 or 100 (^{13}C)] spectrometer, at room temperature for solutions in CDCl_3 .

Chemical shifts are referred to the solvent signal and are expressed in ppm. 2D NMR experiments (COSY, TOCSY, ROESY, and HMQC) were carried out when necessary to assign the corresponding signals of the new compounds. High resolution FAB (+) mass spectral analyses was obtained on a Micromass AutoSpec-Q spectrometer.

2-Hydroxyethyl-2,3,6,2',3',4',6'-hepta-O-acetyl- β -D-maltopyranoside (18). To a solution of hepta-O-acetyl-maltopyranosyl bromide (**17**) (0.80 g, 1.146 mmol) and tetraethylene glycol (4.0 mL, 22.92 mmol, 20 eq.) previously dried over molecular sieves, under argon atmosphere, in anhydrous THF (30 mL) Ag_2CO_3 (3.15 g, 11.46 mmol, 10 eq.) was added and stirring was continued for 22 hours (TLC: Hex-EtOAc, 2:3). The mixture was filtered, diluted with CH_2Cl_2 (100 mL), washed with water (3 x 100 mL), dried over anh. MgSO_4 , and the solvent evaporated under reduced pressure. The product was purified by silica gel column chromatography using as eluent pure EtOAc to EtOAc with 3% methanol to give compound **18** (0.46 g, 50%) as a syrup. ^1H NMR (300 MHz, CDCl_3): δ = 5.34 (d, 1H, J = 3.5 Hz, H-1'), 5.29 (t, 1H, J = 10.0 Hz, H-3'), 5.19 (t, 1H, J = 9.3 Hz, H-3), 4.98 (t, 1H, J = 9.9 Hz, H-4'), 4.81-4.72 (m, 2H, H-2, H-2'), 4.58 (d, 1H, J = 7.8 Hz, H-1), 4.42 (dd, 1H, J = 2.4 and 12.0 Hz, H-6a), 4.21-4.13 (m, 2 H, H-6b, H-6'a), 4.00-3.81 (m, 4 H, H-5, H-5', H-6'b, H-4), 3.71-3.52 (m, 16 H, 4xOCH₂CH₂O), 2.64 (br. s, 1 H, OH), 2.10-1.93 (6s, 21H, OCOCH₃) ppm; ^{13}C NMR (75 MHz, CDCl_3): δ = 170.5, 170.4, 170.2, 170.0, 169.7, 169.4 (C=O), 96.6 (C-1), 94.3 (C-1'), 76.7, 74.4, 73.2, 72.4, 71.1, 70.5, 70.3, 69.0, 69.1, 68.2, 67.0, 62.8, 63.4, 61.5, 21.7, 21.6, 21.4, 21.3, 20.0, 19.9, 19.7, 19.6 ppm; $[\alpha]_D^{22}$ +34.5 (c 1 in CHCl_3); MS (ES^+) Calcd. for $\text{C}_{34}\text{H}_{52}\text{O}_{22}\text{N}_2\text{Na}$: 835.3, found; 835.5.

β -cyanoethoxy- β -(2,3,6,2',3',4',6'-hepta-O-acetyl- β -D-maltopyranosyl)ethoxy diisopropylamine phosphine (19). To a solution of 2-hydroxyethyl-2,3,6,2',3',4',6'-hepta-O-acetyl- β -D-maltopyranoside (**18**) (0.30 g, 0.36 mmol) in dry CH_2Cl_2 (2 mL), DIEA (235 μL , 1.35 mmol) and 2-cyanoethyl-N,N'-diisopropylamino-chlorophosphoramidite (120 μL , 0.54 mmol) were added at room temperature under argon atmosphere. After 2 h, the solution was diluted with EtOAc (25 mL) and the organic phase was washed with brine (3 x 25 mL), dried over anh. MgSO_4 , filtered and the solvent evaporated to dryness.

The product was purified by silica gel column chromatography using as eluent Hex-EtOAc, 1:1 with 5% of NEt₃ to give compound **19** (360 mg, 98%) as a syrup. ¹H NMR (300 MHz, CDCl₃) (mix of isomers): δ = 5.39 (d, 1H, *J* = 3.5 Hz, H-1'), 5.33 (t, 1H, *J* = 10.0 Hz, H-3'), 5.23 (t, 1H, *J* = 9.0 Hz, H-3), 5.03 (t, 1H, *J* = 10.0 Hz, H-4'), 4.85-4.78 (m, 2H, H-2, H-2'), 4.59 (d, 1H, *J* = 8.0 Hz, H-1), 4.46 (m, 1H, H-6a), 4.25-4.18 (m, 2 H, H-6b, H-6'a), 4.03-3.57 (m, 24 H, 4xOCH₂CH₂O, H-5, H-5', H-6'b, H-4, OCH₂CH₂CN, CHisopropyl), 2.65 (m, 2 H, OCH₂CH₂CN), 2.15-2.00 (6s, 21H, OCOCH₃), 1.16 (t, 12 H, CH₃isopropyl) ppm; ¹³C NMR (75 MHz, CDCl₃) (mix of isomers) : δ = 170.5, 170.4, 170.2, 170.0, 169.7, 169.4 (C=O), 117.7 (CN), 100.0 (C-1), 95.3 (C-1'), 75.3, 72.7, 72.1, 71.2, 70.7, 70.6, 70.5, 70.4, 70.1, 70.0, 69.3, 69.1, 68.5, 68.0, 62.8, 62.6, 62.5, 61.5, 58.6, 58.4, 43.1, 42.9, 24.6, 24.5, 20.9, 20.8, 20.7, 20.6, 20.3, 20.2 ppm; ³¹P NMR (101 MHz, CDCl₃): δ= 149.8, 149.7; MS (ES⁺) Calcd. for C₄₃H₆₉O₂₃N₂PNa: 1035.4, found; 1035.0.

2-Hydroxyethyl-O-(2,3,4, 6-tetra-O-acetyl-α-D-glucopyranosyl-(1→4)-O-(2,3,6-tri-O-acetyl-α-D-glucopyranosyl)-(1→4)-2,3,6-tri-O-acetyl-β-D-glucopyranoside (21). To a solution of the deca-*O*-acetyl-maltotriopyranosyl bromide (**20**) (1.69 g, 1.75 mmol) and ethylene glycol (0.98 mL, 17.5 mmol, 10 eq.) previously dried over molecular sieves, under argon atmosphere, in anhydrous CH₂Cl₂ (20 mL) was added Ag₂CO₃ (965 mg, 3.5 mmol, 2.1 eq.). The reaction was then stirred for 24 h. The mixture was then filtered over celite and washed with CH₂Cl₂. The solvent were then removed and the crude was purified by flash column chromatography (hexane: ethyl acetate from 1:3 to 0:1) to afford **21** (1.16 g, 68%) as a glassy solid. ¹H NMR (500 MHz, CDCl₃): δ= 5.34-5.32 (m, 3H, H_{1C}, H_{1B}, H_{3A}), 5.30-5.26 (m, 2H, H_{3B}, H_{4B}), 5.08 (t, 1H, *J* = 10.0 Hz, H_{4C}), 4.88-4.82 (m, 2H, H_{2A}, H_{2C}), 4.75 (dd, 1H, *J* = 4.0 & 10.0 Hz, H_{2B}), 4.59 (d, 1H, *J* = 8.0 Hz, H_{1A}), 4.55 (dd, 1H, *J* = 2.4 & 12.1 Hz, H_{6A}), 4.49-4.46 (m, 1H, H_{6B}), 4.29-4.24 (m, 2H, H_{6'A}, H_{6'B}), 4.21 (dd, 1H, *J* = 3.4 & 12.3 Hz, H_{6C}), 4.06 (m, 1H, H_{6'C}), 4.00-3.92 (m, 4H, H_{5A}, H_{4A}, H_{5B}, H_{5C}), 3.85-3.72 (m, 5H, CH₂O-, CH₂OH, OH), 2.18, 2.16, 2.11, 2.06, 2.04, 2.03, 2.02, 2.015, 2.01, 2.00 (10s, 30H. OCOCH₃) ppm; ¹³C NMR (125 MHz, CDCl₃): δ= 170.7, 170.6, 170.55, 170.5, 170.4, 170.1, 169.9, 169.8, 169.7, 169.4 (C=O), 100.9 (C_{1B}), 95.8 (C_{1A}), 95.7 (C_{1C}), 75.1 (C_{4A}), 73.8, 72.5, 72.3, 72.2, 71.7, 70.4, 70.0, 69.4, 69.0, 68.5, 67.9 (CH), 65.8, 62.8, 62.3, 61.9, 61.8 (C_{6A},

C_{6B}, C_{6C}, OCH₂CH₂OH), 20.9, 20.85, 20.8, 20.7, 20.6, 20.5 (OCOCH₃) PPM; [α]_D²² +39.0 (c 1 in CHCl₃); HRMS (ES⁺) Calcd. for C₃₇H₅₇O₂₀N₂Na: 903.3140, found; 903.3146.

β -Cyanoethoxy- β -[(2,3,4, 6-tetra-O-acetyl- α -D-glucopyranosyl-(1 \rightarrow 4)-O-(2,3,6-tri-O-acetyl- α -D-glucopyranosyl)-(1 \rightarrow 4)-2,3,6-tri-O-acetyl- β -D-glucopyranosyl]ethoxy-diisopropylamine phosphine (22). DIEA (132 μ L, 0.75 mmol) and 2-cyanoethyl-N,N'-diisopropylamino-chlorophosphoramidite (70 μ L, 0.31 mmol) were added to a solution of compound **21** (200 mg, 0.20 mmol) in anhydrous CH₂Cl₂ (4 mL) at room temperature under an argon atmosphere. After 2.0 h no starting material was observed. Solvents were then removed and the crude was purified by silica gel column chromatography by using Hex/EtOAc (1:3 with 5% of NEt₃) to give compound **22** (197 mg, 84%) as a syrup. ¹H NMR (500 MHz, CDCl₃): δ = 5.39-5.17 (m, 5H, H_{1C}, H_{1B}, H_{3A}, H_{3B}, H_{4B}), 5.03 (t, 1H, *J*= 9.9 Hz, H_{4C}), 4.84-4.74 (m, 2H, H_{2A}, H_{2C}), 4.70 (dd, 1H, *J*=3.9 & 10.5 Hz, H_{2B}), 4.59 (m, 1H, H_{1A}), 4.44-4.40 (m, 1H, H_{6A}, H_{6B}), 4.30-3.44 (m, 16H, H_{6'A}, H_{6'B}, H_{6C}, H_{6'C}, H_{5A}, H_{4A}, H_{5B}, H_{5C}, CH₂O-, CH₂CH₂CN, CH₂OH, CH_{isopropyl}), 2.60 (m, 2 H, OCH₂CH₂CN), 2.14, 2.12, 2.06, 2.01, 1.99, 1.98, 1.96, 1.94 (8s, 30H, OCOCH₃), 1.20-1.14 (m, 12 H, CH_{3isopropyl}) ppm; ¹³C NMR (125 MHz, CDCl₃): δ = 170.5, 170.5, 170.4, 170.3, 170.1, 169.8, 169.7, 169.4 (C=O), 117.7 (CN), 100.2 (C_{1B}), 95.7 (C_{1A}), 95.6 (C_{1C}), 75.3 (C_{4A}), 73.8, 72.4, 72.0, 71.7, 70.4, 70.0, 69.4, 69.3, 68.8, 68.4, 67.8 (CH), 63.0, 62.3, 61.3, 58.6, 58.3 (C_{6A}, C_{6B}, C_{6C}, OCH₂CH₂OH), 45.1, 45.0, 43.1, 42.9, 24.7, 24.6, 24.5, 22.9, 20.9, 20.8, 20.7, 20.6 (OCOCH₃) PPM; ³¹P NMR (101 MHz, CDCl₃): δ = 149.8, 149.6; HRMS (ES⁺) Calcd. for C₄₉H₇₄N₂O₂₈P (M+H): 1169.4166, found; 1169.4188.

Synthesis of carbohydrate oligonucleotide conjugates. Oligodeoxynucleotides carrying carbohydrates at the 5'-end were prepared in a DNA synthesizer (*Applied Biosystems 3400*) using standard 2-cyanoethyl phosphoramidites and the appropriate carbohydrate phosphoramidites (Schemes 1 and 2). The syntheses were carried out on controlled-pore-glass (CPG) supports carrying the 2-(*N*-[9H-fluoren-9-yl-methoxycarbonyl]-4-aminobutyl)propane-1,3-diol linker (*Glen Research*) to yield oligonucleotides carrying an aliphatic amino group at the 3'-end (27). The following sequences were prepared: Sequence **1**: CTCTCGCACCCATCTCTCTCCTTCT-3'-NH₂; sequence **2**: Glucose-C2-5'-

CTCTCGCACCCATCTCTCTCCTTCT-3'-NH₂, (C2 stands for -CH₂CH₂-OPO₂⁻); sequence **3**:
 Fucose-C2-5'-CTCTCGCACCCATCTCTCTCCTTCT-3'-NH₂; sequence **4**: (Glucose-C2)₂-DB-
 CTCTCGCACCCATCTCTCTCCTTCT-3'-NH₂; DB stands for the symmetric doubler phosphoramidite
 obtained from commercial sources (*Glen Research*); sequence **5**: (Glucose-C2)₄-DB-DB-
 CTCTCGCACCCATCTCTCTCCTTCT-3'-NH₂; sequence **6**: Maltose-PEG4-5'-
 CTCTCGCACCCATCTCTCTCCTTCT-3'-NH₂, (PEG4 stands for -(OCH₂CH₂)₄-OPO₂⁻); sequence **7**:
 Maltotriose-C2-5'-CTCTCGCACCCATCTCTCTCCTTCT-3'-NH₂. After ammonia deprotection
 (overnight, 55 °C) the resulting oligodeoxynucleotides were purified by HPLC (see conditions below).
 The purified products were analyzed by MALDI-TOF mass spectrometry. Sequence **1** [M] = 7603.6
 (expected M= 7600.0). Yield (1 μmol scale synthesis) was 118 OD units at 260 nm (580 nmol, 58%).
 Sequence **2** [M] = 7888.4 (expected M= 7886.2). Yield (1 μmol scale synthesis) was 83 OD units at 260
 nm (410 nmol, 41%). Sequence **3** [M] = 7870.7 [(expected M= 7870.7). Yield (1 μmol scale synthesis)
 was 98 OD units at 260 nm (480 nmol, 48%). Sequence **4** [M] = 8484.5 (expected M= 8522.9). Yield
 (0.5 μmol scale synthesis) was 31 OD units at 260 nm (155 nmol, 31%). Sequence **5** [M] = 9755.1 [
 (expected M= 9795.8). Yield (0.5 μmol scale synthesis) was 23 OD units at 260 nm (115 nmol, 23%).
 Sequence **6** [M] = 8180.7 [(expected M= 8182.7). Yield (0.5 μmol scale synthesis) was 22.5 OD units at
 260 nm (110 nmol, 22%). Sequence **7** [M] = 8210.7 [(expected M= 8210.7). Yield (0.5 μmol scale
 synthesis) was 28 OD units at 260 nm (140 nmol, 28%).

Synthesis of carbohydrate oligonucleotide conjugates carrying fluorescent label. The following
 sequences were prepared: sequence **8**: CTCTCGCACCCATCTCTCTCCTTCT-3'-NHCO-Alexa488;
 sequence **9**: Glucose-C2-5'-CTCTCGCACCCATCTCTCTCCTTCT-3'-NHCO-Alexa488; sequence **10**:
 Fucose-C2-5'-CTCTCGCACCCATCTCTCTCCTTCT-3'-NHCO-Alexa488; sequence **11**: (Glucose-
 C2)₂-DB-CTCTCGCACCCATCTCTCTCCTTCT-3'-NHCO-Alexa488; sequence **12**: (Glucose-C2)₄-
 DB-DB-CTCTCGCACCCATCTCTCTCCTTCT-3'-NHCO-Alexa488; sequence **13**: Maltose-PEG4-5'-
 CTCTCGCACCCATCTCTCTCCTTCT-3'-NHCO-Alexa488; sequence **14**: Maltotriose-C2-5'-

CTCTCGCACCCATCTCTCTCCTTCT-3'-NHCO-Alexa488. Carbohydrate oligonucleotide conjugates carrying the fluorescent label at the 3'-end were prepared by reaction of the corresponding 3-amino oligonucleotides (**1-7**) with Alexa Fluor® 488 tetrafluorophenyl (5-TPF) ester obtained from commercial sources (*Invitrogen*). The corresponding 3'-amino-oligonucleotide was dissolved with 50 µL of an aqueous solution of 0.2M NaHCO₃ (pH=9). Then, 1.1 equivalents of Alexa Fluor® 488 5-TPF dissolved in 30 µL DMF were added to the solution and left to react overnight at room temperature. The mixture was concentrated to dryness, and the residue was dissolved in H₂O. The residue was dissolved with 1 mL H₂O and was purified with *Sephadex G-25 (NAP-10 Column)* and the oligonucleotide fraction was analyzed by HPLC (see conditions below). The purified products were analyzed by MALDI-TOF mass spectrometry. Sequence **8** [M] = 8117.4 (expected M= 8166.5). Yield (0.23 µmol scale) was 43 OD units at 260 nm (93%). Sequence **9** [M] = 8400.0 (expected M= 8402.7). Yield (0.21 µmol scale) was 42 OD units at 260 nm (93%). Sequence **10** [M] = 8378.6 (expected M= 8386.7). Yield (0.25 µmol scale) was 44 OD units at 260 nm (86%). Sequence **11** [M] = 9037.9 (expected M= 9009.5). Yield (0.07 µmol scale synthesis) was 15 OD units at 260 nm (67%). Sequence **12** [M] = 10280.3 (expected M= 10310.8). Yield (0.07 µmol scale) was 23 OD units at 260 nm (87%). Sequence **13** [M] = 8664.3 (expected M= 8695.7). Yield (0.06 µmol scale) was 13 OD units at 260 nm (61%). Sequence **14** [M] = 8698.4 (expected M= 8695.7). Yield (0.1 µmol scale) was 19 OD units at 260 nm (90%).

HPLC purification conditions. Column: Nucleosil 120C₁₈ (10µm, 200x10 mm). Flow rate: 3 mL/min. Conditions: 20 min. linear gradient from 0-50% B. The purity of the resulting oligonucleotides was analyzed as follows: Column: X-Bridge™OST C₁₈ (2.5 µm 4.6x50 mm). Flow rate: 1 mL/min. Conditions: 10 min. linear gradient from 0-30% B). In both cases, solvent A: 5% acetonitrile in 100 mM triethylammonium acetate (pH=7) and solvent B: 70% acetonitrile in 100 mM triethylammonium acetate (pH=7).

Mass spectrometry. MALDI-TOF spectra were performed using a *Perseptive Voyager DETMRP* mass spectrometer, equipped with nitrogen laser at 337 nm using a 3ns pulse. The matrix used contained

2,4,6-trihydroxyacetophenone (THAP, 10 mg/ml in ACN/ water 1:1) and ammonium citrate (50 mg/ ml in water).

Cell cultures. HeLa (cervical carcinoma) and U87.CD4.CXCR4 cells lines were kindly provided by Prof. Alfredo Berzal (Instituto de Parasitología y Biomedicina “López-Neyra”, CSIC, Granada, Spain). Cells were cultured as exponentially growing subconfluent monolayers and maintained in Dulbecco’s modified Eagle’s medium (DMEM, PAA Laboratories GMBH) supplemented with 10 % Fetal Bovine Serum (FBS, Invitrogen), 4 mM L-Glutamine (Sigma), Mycokill AB (PAA Laboratories GMBH) and penicillin/streptomycin (100 units/ml and 100 µg/ml, respectively) (Invitrogen) in a humidified atmosphere consisting of 5% CO₂ and 95% air. Human astroglioma U87.CD4.CXCR4 cells were also supplemented with 1 µg/ml puromicine (Sigma) and 300 µg/ml geneticin (G-418 sulphate) (Invitrogen).

Cell-surface adsorption studies by flow cytometric analysis. Cells were seeded into 24-well plates 48 hours prior to treatment in DMEM supplemented with 10% FBS, in the absence or presence of glucose (5.5 mM glucose). Then, cells were incubated on ice serum-free DMEM containing 5 µM of different Alexa 488-labelled oligonucleotides, in the absence or presence (5.5 mM) of glucose for 1 h, washed twice with ice-cold phosphate-buffered saline (PBS), harvested and resuspended in ice-cold PBS, followed by a flow cytometry analysis (FACSCalibur, Beckton Dickinson).

Cellular uptake studies by flow cytometric analysis. Cells were seeded into 24-well plate prior to treatment in DMEM supplemented with 10% FBS and 5.5 mM glucose. Then, cells were incubated with 2 µM of different Alexa 488-labelled oligonucleotides at 37°C in the presence or absence of glucose for 2, 6 and 24 h. After incubation, cells were completely dissociated in 0.5% Trypsin-EDTA (Invitrogen). Trypsin treated cells were washed by centrifugation at 520xg for 10 min and then resuspended into ice-cold 1X PBS, followed by a flow cytometry analysis. The fluorescence of Alexa-labelled oligonucleotides remaining at the cellular surface was quenched with 0.2% Trypan Blue (final concentration) and subsequently, the fluorescence corresponding to the internalized oligonucleotides was measured.

RESULTS AND DISCUSSION

Synthesis of carbohydrate phosphoramidites (15, 16, 19, 22). Among the different approaches described to prepare carbohydrate oligonucleotide conjugates (COCs) (21), we selected one of the most straightforward methodologies based on the coupling of a sugar phosphoramidite to oligonucleotides on a solid support. This approach has been previously used to introduce sugars linked through the primary alcohol (28, 29) where the anomeric position was methylated. Our group (30) and others (31) have used this methodology to introduce sugars linked through the anomeric position. We have extended this approach to prepare COCs that possess a glucose moiety with different presentations. With this purpose we have attached sugars to DNA strands through two types of spacers (ethylene glycol, C2 or tetraethyleneglycol, PEG4) and a commercially available symmetric dendrimer (symmetric doubler phosphoramidite). Glucose and fucose phosphoramidites (**15** and **16**, respectively) carrying the short spacers were recently synthesized in two steps (30): classical glycosylation from their corresponding bromo peracetylated sugars and ethylene glycol and subsequent standard phosphoramidite chemistry (Scheme 1). Following the same strategy maltose and maltotriose phosphoramidites have been prepared carrying tetraethylene glycol and ethylene glycol spacers, respectively (compounds **19** and **22**, Scheme 2). Glycosylation was carried out using silver carbonate as the promoter to obtain moderate yields of intermediates **18** and **21** (50 and 68%, respectively). The resulting alcohols were reacted with 2-cyanoethyl N,N-diisopropylchlorophosphoramidite and N-diisopropylethylamine to yield the carbohydrate phosphoramidite derivatives **19** and **22** (84 and 98%, respectively).

Synthesis of carbohydrate oligonucleotide conjugates (2-7). Oligodeoxynucleotides carrying carbohydrates at the 5'-end were prepared using the appropriate carbohydrate phosphoramidites (Schemes 1 and 2) and the commercial dendrimer symmetric doubler phosphoramidite. We selected the well-known antisense oligonucleotide sequence GEM91 (5'-CTCTCGCACCCATCTCTCTCCTTCT) that was targeted to the translational initiation site of the Gag mRNA of HIV (32). We designed oligonucleotide sequences that carried an amino group at the 3'-end so that a carboxyl-activated

fluorescent label could be attached at a subsequent step. We selected the commercially available 3'-amino-modifier C7 CPG for the amino modification of the COC's. The oligonucleotide glycoconjugates (**2-7**) contained the following carbohydrates covalently linked to the GEM91 oligonucleotide with different spacers: glucose-ethylene glycol, fucose-ethylene glycol as control, maltose-tetraethylene glycol, maltotriose-ethylene glycol, di-glucose-doubler dendrimer and tetra-glucose-doubler-doubler dendrimer, respectively. Additionally, a non-conjugated 3-amino oligonucleotide (**1**) was synthesized for reference. Oligonucleotides **1**, **2** and **3** show a single peak (Figure 2) that had the expected mass and they were used in the next reaction without further purification (41-58% yield). Oligonucleotides **4-7** presented a major peak with some impurities (Figure 2) that were easily separated by HPLC obtaining the desired conjugates in a 22-31% yield after HPLC purification. The side products from the synthesis of the branched oligonucleotides **4** and **5** were collected and analyzed by MS and gel electrophoresis showing that these side products lack one or two glucose residues. This confirms that phosphoramidite couplings after branching are somehow less efficient according to literature (33, 34) but this fact did not prevent obtaining pure oligonucleotide conjugates with two and four glucose units.

Synthesis of carbohydrate oligonucleotide conjugates carrying a fluorescent label (9-14). For the cellular uptake studies, six 3'-end fluorescently labelled oligonucleotide glycoconjugates (**9-14**) were prepared. We selected Alexa 488 as the fluorescent tag due to its brightness compared to other common fluorescent labels, its fluorescent life time and the hydrolytic stability of the corresponding amine-reactive Alexa 488 derivative. These compounds contained the same carbohydrate moieties presented above. Carbohydrate oligonucleotide conjugates (**2-7**) dissolved in 0.1–0.2 M sodium bicarbonate buffer (pH 8.3) were reacted with Alexa Fluor® 488 tetrafluorophenyl ester dissolved in DMF for 1 h at room temperature. In all cases a major peak was obtained (Figure 3) and the desired fluorescently labeled oligonucleotides were isolated in good yields (67-93%). Finally, a control labelled DNA oligonucleotide (**8**) was prepared using the same conditions described above.

Cell-surface adsorption and uptake by flow cytometric analysis. We measured cell-surface adsorption of the carbohydrate oligonucleotide conjugates (**9-14**, **Fig. 1**) and the control labeled DNA oligonucleotide (**8**, **Fig. 1**) both in the presence and absence of glucose in the medium. HeLa cells and U87.CD4.CXCR4 cells were seeded on 24-well culture plates, in the presence (5.5 mM) or absence of glucose for 48 h until preconfluency at 37 °C. Then, the medium was replaced and cells were incubated with 5 µM bioconjugate for 1 h at 4 °C in the presence or absence of glucose. Note that incubation at 4 °C allows oligonucleotide adsorption onto the cell-surface but not endocytosis-dependent cellular internalization (35). After incubation cells were washed and resuspended in ice-cold PBS and analyzed by flow cytometry (Figure 4). In the absence of glucose, an overall increase in fluorescence intensity is observed for all the oligonucleotides analyzed in comparison to the data observed when glucose was present in the medium. This behavior was similar for both HeLa and U87.CD4.CXCR4 cells and it could be due to the starving conditions suffered by the cells during long periods of time (*i.e.*, 48 h). In general, although there are only small differences among all the oligonucleotides analyzed, a slight increment in fluorescence could be observed for oligonucleotides **11** and **13**, for both cell types in the presence or absence of glucose.

To determine the influence of glucose units in the oligonucleotide and the relevance of the different spatial presentation in the cellular uptake, the carbohydrate oligonucleotide conjugates labeled with Alexa 488 (**9-14**, **Fig. 1**) and the control labeled DNA oligonucleotide (**8**, **Fig. 1**) were incubated with HeLa cells and U87.CD4.CXCR4 cells. The incubation was performed under standard conditions with 2 µM oligonucleotide for 2 h at 37 °C, both in the absence and in the presence of glucose (5.5 mM). After washing the fluorescence intensity was determined by flow cytometry (Figure 5). Flow cytometry revealed that the fluorescence intensity of the cells was higher for DNA glycoconjugates **11** and **13** than for glycoconjugates **9**, **10**, **12**, **14** and the control labeled DNA oligonucleotide without sugar modification **8**. This behavior was observed both in HeLa and U87.CD4.CXCR4 cells (**Fig. 5, A and B**), in the absence or presence of glucose, these differences being much smaller when glucose was present in the medium. It seems that oligonucleotides with the glucose moiety linked through longer spacers (15

and 18 atom distance in COC's **11** and **13**, respectively) showed better incorporation into the target cell than those with glucose linked through shorter spacers (4 atom distance in COC **9**). Moreover, high multivalency of glucose, as in glycoconjugate **14**, seems to hinder cell uptake maybe due to its high structural volume.

CONCLUSIONS

We have efficiently synthesized carbohydrate oligonucleotide conjugates with sugar moieties bound at the 5'-end of the DNA strand obtaining good yields and purities. Two types of spacers, ethylene glycol and tetraethylene glycol, and a doubler dendrimer were used to construct DNA glycoconjugates with different glucose presentations. Cellular uptake of oligonucleotides containing a terminal glucose unit linked through a long tetraethyleneglycol spacer or just one doubler dendrimer was more efficient than the other glycoconjugates and the unconjugated control. In contrast, the conjugate containing four glucose units showed lower cell uptake, both in HeLa and U87.CD4.CXCR4 cells. These results indicate that keeping a certain distance (15 to 18 atoms) between DNA and sugar modification could be important for a better incorporation of the oligonucleotide conjugate into the target cell. In fact, this strategy seems promising for further DNA conjugate design.

ACKNOWLEDGMENT

This work was supported by Consejo Superior de Investigaciones Científicas (PIF06-045); Spanish Ministry of Education (grants BFU2007-63287, BFU2007-62062, CTQ2006-01123/BQU), Generalitat de Catalunya (2009/SGR/208), and Instituto de Salud Carlos III (CIBER-BNN, CB06_01_0019). RL thanks CSIC for a JAE contract.

Supporting Information available: NMR spectral data for compounds **18**, **19**, **21** and **22**. This material is available free of charge via the internet at <http://pubs.acs.org>.

Figure Captions

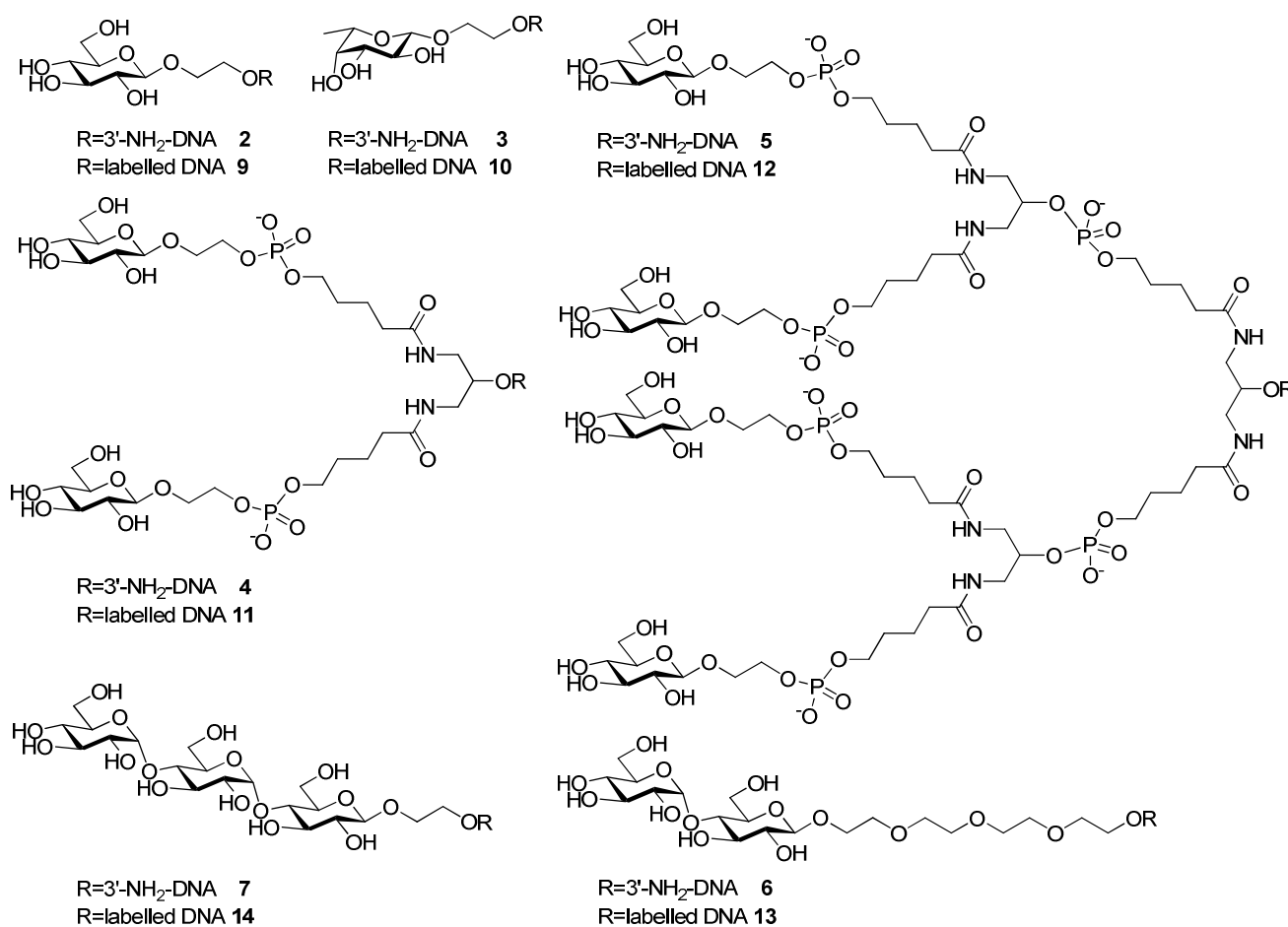
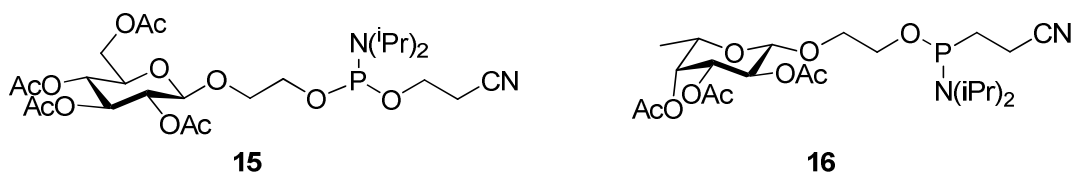
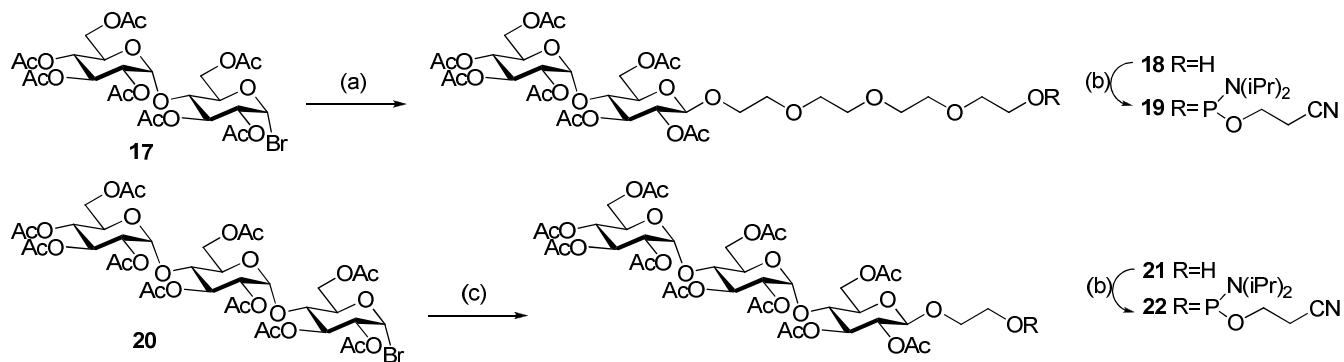


Figure 1. Carbohydrate oligonucleotide conjugates prepared (**2-7** and **9-14**). 3'-NH₂-DNA strands corresponds to -OPO₂⁻-GEM91-3'-NH₂ sequence (GEM91= CTCTCGCACCCATCTCTCTCCTTCT); the corresponding DNA control **1** is the sequence GEM91-3'-NH₂. *Labelled DNA* corresponds to GEM91 strands with Alexa 488 coupled at the 3'-end; the corresponding labelled DNA control **8** is the sequence GEM91-3'-NHCO-Alexa 488.



Scheme 1. Carbohydrate phosphoramidites **15** and **16**.



Scheme 2. Synthetic route used to prepare the carbohydrate phosphoramidite derivatives **19** and **22**. (a) tetraethylene glycol, Ag_2CO_3 , THF, r.t., 22h, 50%; (b) 2-cyanoethyl-*N,N'*-diisopropylamino-chlorophosphoramidite, DIEA, CH_2Cl_2 , r.t., 2h, 84-98%; (c) ethylene glycol, Ag_2CO_3 , CH_2Cl_2 , r.t., 18h, 68%.

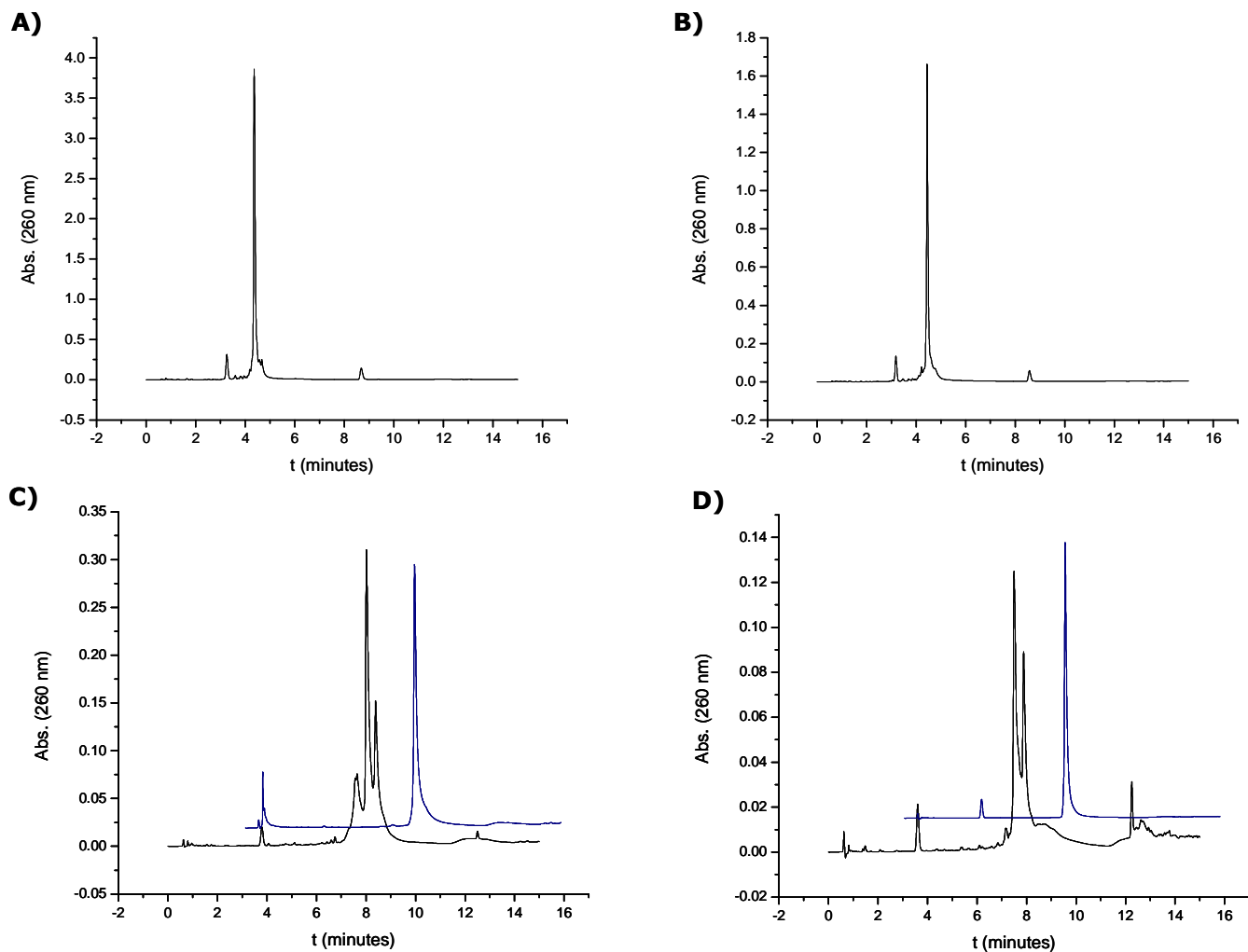


Figure 2. HPLC profiles of 3'-amino 5'-carbohydrate oligonucleotide conjugates: **A)** glucose conjugate **2**, **B)** fucose conjugate **3**, **C)** diglucose conjugate **4** and **D)** tetraglucose conjugate **5**. Insets in **C)** and **D)** correspond to the analytical HPLC profiles of purified conjugates using X-Bridge TMOST C18 columns.

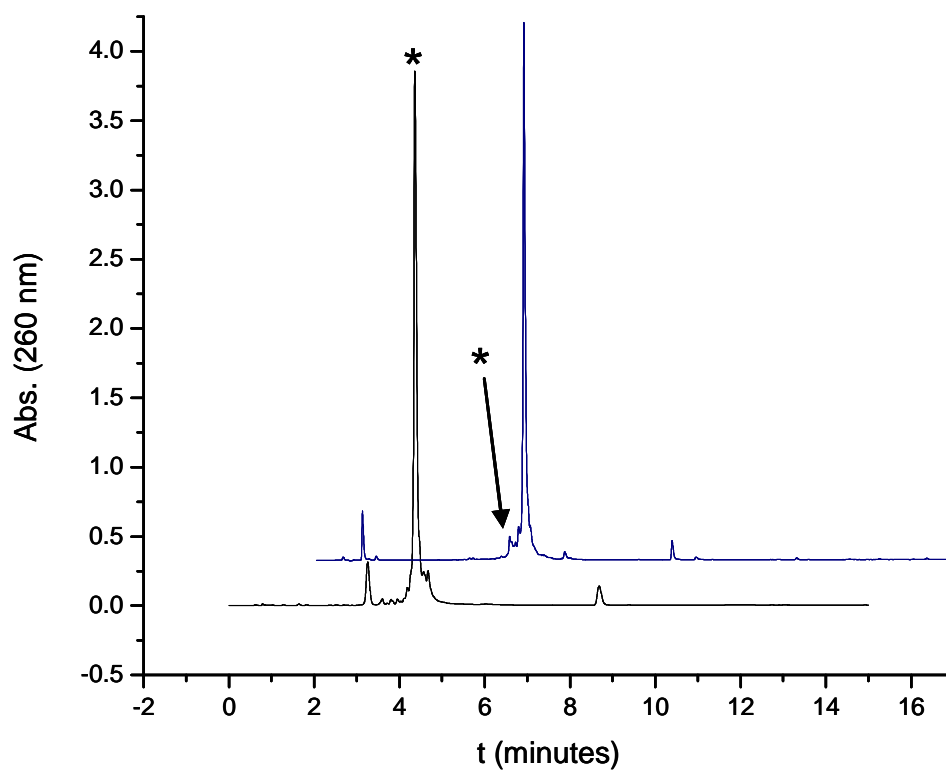


Figure 3. HPLC profiles of glucose conjugate **2** (below), and reaction mixture of **2** with Alexa 488 (above) showing the formation of the 3'-Alexa 5'-glucose conjugate **9**. The asterisk indicates the position of the starting amino oligonucleotide **2**. Column: X-Bridge TMOST C18 (2.5 mm 4.6x50 mm). Flow rate: 1 mL/min. Conditions: 10 min. linear gradient from 0-30%.

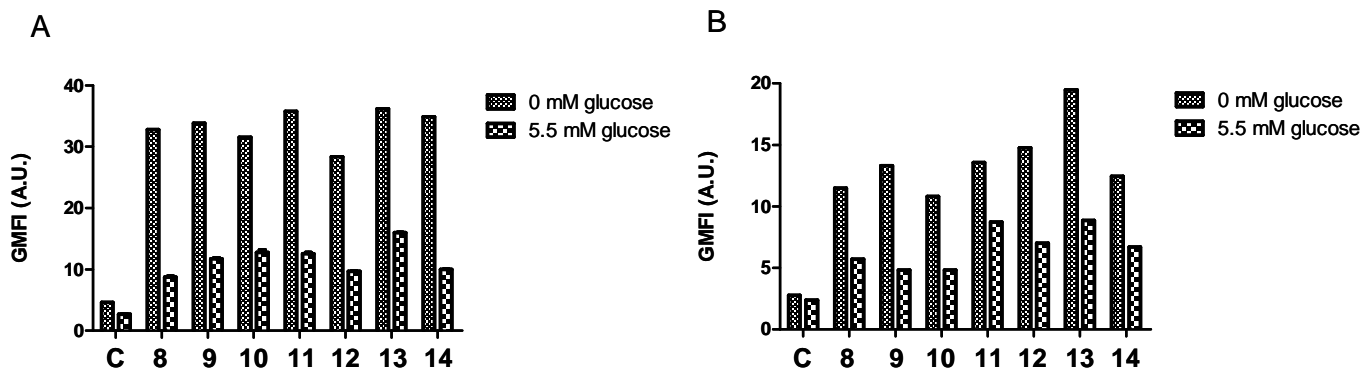


Figure 4. Cell-surface adsorption of Alexa 488-labeled carbohydrate oligonucleotide conjugates (**9-14**) and control Alexa 488-labeled DNA oligonucleotide **8**. (A) HeLa cells and (B) U87.CD4.CXCR4 cells were cultured in the absence or presence of glucose for 48 h at 37 °C. Then, the medium was replaced and cells were incubated with 5 μ M bioconjugate for 1 h at 4 °C in the absence or presence of glucose. After incubation, cells were washed three times, resuspended in ice-cold PBS and analyzed by flow cytometry. C represents cell basal fluorescence intensity. GMFI corresponds to Geometric Mean of Fluorescence Intensity. Measurements from two independent experiments were averaged. Error bars indicate S.D.

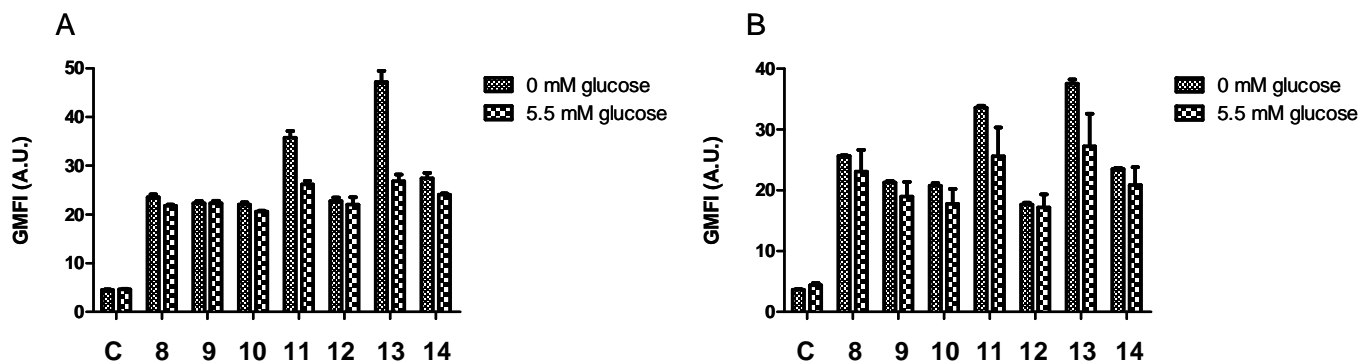


Figure 5. Cellular uptake of Alexa 488-labeled carbohydrate oligonucleotide conjugates (9-14) and control Alexa 488-labeled DNA oligonucleotide 8. (A) HeLa cells and (B) U87.CD4.CXCR4 cells were cultured until preconfluency at 37 °C. Then, the medium was replaced and cells were incubated with 2 μ M bioconjugate for 2 h at 37 °C in the absence or presence of glucose. After incubation, cells were washed three times, resuspended in ice cold PBS and analyzed by flow cytometry. C represents cell basal fluorescence intensity. GMFI corresponds to Geometric Mean of Fluorescence Intensity. Measurements from three independent experiments were averaged. Error bars indicate S.D.

LITERATURE CITED

- (1) Braasch, D. A., and Corey, D. R. (2002) Novel antisense and peptide nucleic acid strategies for controlling gene expression. *Biochemistry* 41, 4503-10.
- (2) Fabani, M. M., Turner, J. J., and Gait, M. J. (2006) Oligonucleotide analogs as antiviral agents. *Curr Opin Mol Ther* 8, 108-14.
- (3) Aboul-Fadl, T. (2005) Antisense oligonucleotides: the state of the art. *Curr Med Chem* 12, 2193-214.
- (4) Chan, J. H., Lim, S., and Wong, W. S. (2006) Antisense oligonucleotides: from design to therapeutic application. *Clin Exp Pharmacol Physiol* 33, 533-40.
- (5) Frank-Kamenetskii, M. D., and Mirkin, S. M. (1995) Triplex DNA structures. *Annu Rev Biochem* 64, 65-95.
- (6) Praseuth, D., Guieysse, A. L., and Helene, C. (1999) Triple helix formation and the antigene strategy for sequence-specific control of gene expression. *Biochim Biophys Acta* 1489, 181-206.
- (7) Sun, J. S., Garestier, T., and Helene, C. (1996) Oligonucleotide directed triple helix formation. *Curr Opin Struct Biol* 6, 327-33.
- (8) Bumcrot, D., Manoharan, M., Koteliansky, V., and Sah, D. W. Y. (2006) RNAi therapeutics: a potential new class of pharmaceutical drugs. *Nat Chem Biol* 2, 711-719.
- (9) de Fougerolles, A., Manoharan, M., Meyers, R., and Vornlocher, H. P. (2005) RNA interference in vivo: toward synthetic small inhibitory RNA-based therapeutics. *Methods Enzymol* 392, 278-96.
- (10) Sioud, M., and Iversen, P. O. (2005) Ribozymes, DNazymes and small interfering RNAs as therapeutics. *Curr Drug Targets* 6, 647-53.
- (11) Santel, A., Aleku, M., Keil, O., Endruschat, J., Esche, V., Durieux, B., Loffler, K., Fechtner, M., Rohl, T., Fisch, G., Dames, S., Arnold, W., Giese, K., Klippel, A., and Kaufmann, J. (2006) RNA interference in the mouse vascular endothelium by systemic administration of siRNA-lipoplexes for cancer therapy. *Gene Ther* 13, 1360-1370.
- (12) Kim, S. H., Mok, H., Jeong, J. H., Kim, S. W., and Park, T. G. (2006) Comparative evaluation of target-specific GFP gene silencing efficiencies for antisense ODN, synthetic siRNA, and siRNA plasmid complexed with PEI-PEG-FOL conjugate. *Bioconjug Chem* 17, 241-4.
- (13) Urban-Klein, B., Werth, S., Abuharbeid, S., Czubayko, F., and Aigner, A. (2004) RNAi-mediated gene-targeting through systemic application of polyethylenimine (PEI)-complexed siRNA in vivo. *Gene Ther* 12, 461-466.
- (14) Mok, H., and Park, T. G. (2008) Self-crosslinked and reducible fusogenic peptides for intracellular delivery of siRNA. *Biopolymers* 89, 881-888.
- (15) Park, T. G., Jeong, J. H., and Kim, S. W. (2006) Current status of polymeric gene delivery systems. *Adv Drug Delivery Rev* 58, 467-486.
- (16) Lonnberg, H. (2009) Solid-phase synthesis of oligonucleotide conjugates useful for delivery and targeting of potential nucleic acid therapeutics. *Bioconjugate Chem* 20, 1065-94.
- (17) Jeong, J. H., Mok, H., Oh, Y. K., and Park, T. G. (2009) siRNA conjugate delivery systems. *Bioconjug Chem* 20, 5-14.
- (18) LeDoan, T., Eto, F., Tenu, J. P., Letourneux, Y., and Agrawal, S. (1999) Cell binding, uptake and cytosolic partition of HIV anti-gag phosphodiester oligonucleotides 3'-linked to cholesterol derivatives in macrophages. *Bioorg Med Chem* 7, 2263-9.
- (19) Soutschek, J., Akinc, A., Bramlage, B., Charisse, K., Constien, R., Donoghue, M., Elbashir, S., Geick, A., Hadwiger, P., Harborth, J., John, M., Kesavan, V., Lavine, G., Pandey, R. K., Racie, T., Rajeev, K. G., Rohl, I., Toudjarska, I., Wang, G., Wuschko, S., Bumcrot, D., Koteliansky, V., Limmer, S., Manoharan, M., and Vornlocher, H. P. (2004) Therapeutic silencing of an endogenous gene by systemic administration of modified siRNAs. *Nature* 432, 173-8.

- (20) Zelphati, O., Wagner, E., and Leserman, L. (1994) Synthesis and anti-HIV activity of thiocholesteryl-coupled phosphodiester antisense oligonucleotides incorporated into immunoliposomes. *Antiviral Res* 25, 13-25.
- (21) Yan, H., and Tram, K. (2007) Glycotargeting to improve cellular delivery efficiency of nucleic acids. *Glycoconj J* 24, 107-23.
- (22) Zatsepin, T. S., and Oretskaya, T. S. (2004) Synthesis and applications of oligonucleotide-carbohydrate conjugates. *Chem Biodivers* 1, 1401-17.
- (23) Karskela, M., Virta, P., Malinen, M., Urtti, A., and Lonnberg, H. (2008) Synthesis and cellular uptake of fluorescently labeled multivalent hyaluronan disaccharide conjugates of oligonucleotide phosphorothioates. *Bioconjugate Chem* 19, 2549-58.
- (24) Ye, Z., Cheng, K., Guntaka, R. V., and Mahato, R. I. (2005) Targeted delivery of a triplex-forming oligonucleotide to hepatic stellate cells. *Biochemistry* 44, 4466-76.
- (25) Zhu, L., Ye, Z., Cheng, K., Miller, D. D., and Mahato, R. I. (2008) Site-specific delivery of oligonucleotides to hepatocytes after systemic administration. *Bioconjugate Chem* 19, 290-8.
- (26) Oishi, M., Nagasaki, Y., Itaka, K., Nishiyama, N., and Kataoka, K. (2005) Lactosylated poly(ethylene glycol)-siRNA conjugate through acid-labile beta-thiopropionate linkage to construct pH-sensitive polyion complex micelles achieving enhanced gene silencing in hepatoma cells. *J Am Chem Soc* 127, 1624-5.
- (27) Nelson, P. S., Kent, M., and Muthini, S. (1992) Oligonucleotide labeling methods 3. Direct labeling of oligonucleotides employing a novel, non-nucleosidic, 2-aminobutyl-1,3-propanediol backbone. *Nucleic Acids Res.* 20, 6253-6259.
- (28) Katajisto, J., Heinonen, P., and Lonnberg, H. (2004) Solid-phase synthesis of oligonucleotide glycoconjugates bearing three different glycosyl groups: orthogonally protected bis(hydroxymethyl)-N,N'-bis(3-hydroxypropyl)malondiamide phosphoramidite as key building block. *J Org Chem* 69, 7609-15.
- (29) Wang, Y., and Sheppard, T. L. (2003) Chemoenzymatic synthesis and antibody detection of DNA glycoconjugates. *Bioconjugate Chem* 14, 1314-22.
- (30) Morales, J. C., Reina, J., J., Díaz, I., Aviñó, A., Nieto, P. M., and Eritja, R. (2008) Experimental Measurement of Carbohydrate-Aromatic Stacking in Water by Using a Dangling-Ended DNA Model System. *Chem - Eur J* 14, 7828-7835.
- (31) Akhtar, S., Routledge, A., Patel, R., and Gardiner, J. M. (1995) Synthesis of mono- and dimannoside phosphoramidite derivatives for solid-phase conjugation to oligonucleotides. *Tetrahedron Lett* 36, 7333-7336.
- (32) Lisiewicz, J., Sun, D., Weichold, F. F., Thierry, A. R., Lusso, P., Tang, J., Gallo, R. C., and Agrawal, S. (1994) Antisense oligodeoxynucleotide phosphorothioate complementary to Gag mRNA blocks replication of human immunodeficiency virus type 1 in human peripheral blood cells. *Proc Nat Acad Sci USA* 91, 7942-7946.
- (33) Aviñó, A., Grimau, M. G., Frieden, M., and Eritja, R. (2004) Synthesis and Triple-Helix-Stabilization Properties of Branched Oligonucleotides Carrying 8-Aminoadenine Moieties. *Helv Chim Acta* 87, 303-316.
- (34) Grimau, M. G., Iacopino, D., Aviñó, A., de la Torre, B. G., Ongaro, A., Fitzmaurice, D., Wessels, J., and Eritja, R. (2003) Synthesis of Branched Oligonucleotides as Templates for the Assembly of Nanomaterials. *Helv Chim Acta* 86, 2814-2826.
- (35) Nishi, K., and Saigo, K. (2007) Cellular internalization of green fluorescent protein fused with herpes simplex virus protein VP22 via a lipid raft-mediated endocytic pathway independent of caveolae and Rho family GTPases but dependent on dynamin and Arf6. *J Biol Chem* 282, 27503-17.

Supporting Information

Synthesis, cell-surface binding and cellular uptake of fluorescently labelled glucose DNA conjugates with different carbohydrate presentation

*Begoña Ugarte-Uribe,[§] Sónia Pérez-Rentero,[‡] Ricardo Lucas,[†] Anna Aviñó,[‡] José J. Reina,[†] Itziar
Alkorta,[§] Ramón Eritja,[‡] Juan C. Morales^{*,†}*

[§] Unidad de Biofísica, Centro Mixto CSIC-UPV/EHU, Universidad del País Vasco, Bilbao, Spain.

[‡] Institute for Research in Biomedicine (IRB Barcelona), Institute for Advanced Chemistry of Catalonia (IQAC-CSIC), Networking Centre on Bioengineering, Biomaterials and Nanomedicine (CIBER-BBN), Edifici Helix, Baldiri Reixac 15, E-08028 Barcelona, Spain.

[†] Instituto de Investigaciones Químicas, CSIC – Universidad de Sevilla, 49 Americo Vesputio, 41092 Sevilla, Spain.

*To whom the corresponding should be addressed: Dr. Juan C. Morales

Phone: +34-954-489561, Fax: +34-954-456505

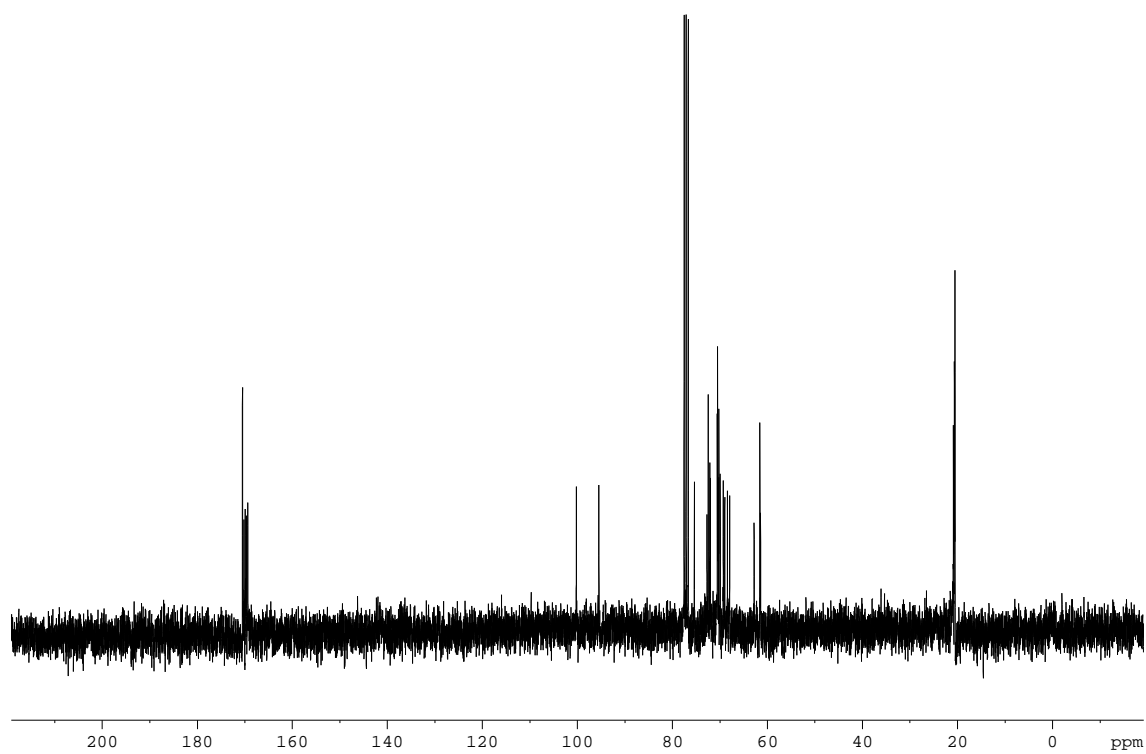
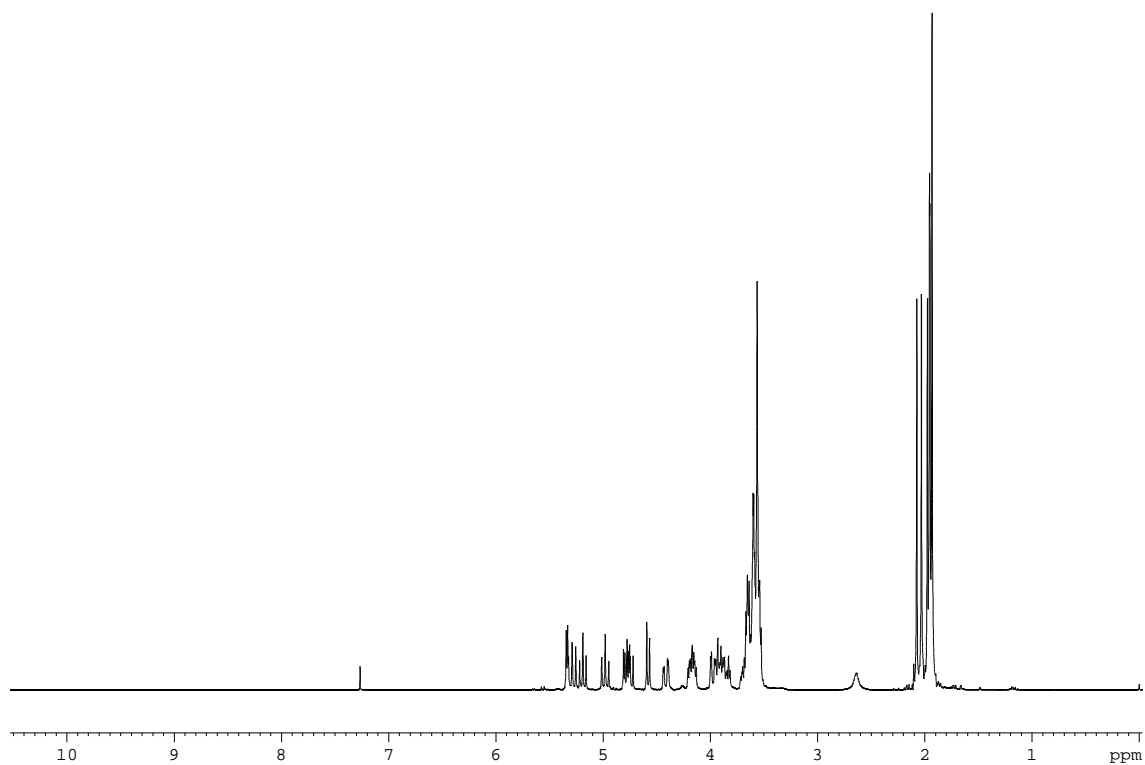
E-mail: jcmorales@iiq.csic.es

Contents

¹H-NMR and ¹³C-NMR spectra of compounds **18**, **19**, **21** and **22**. Pages 2-5

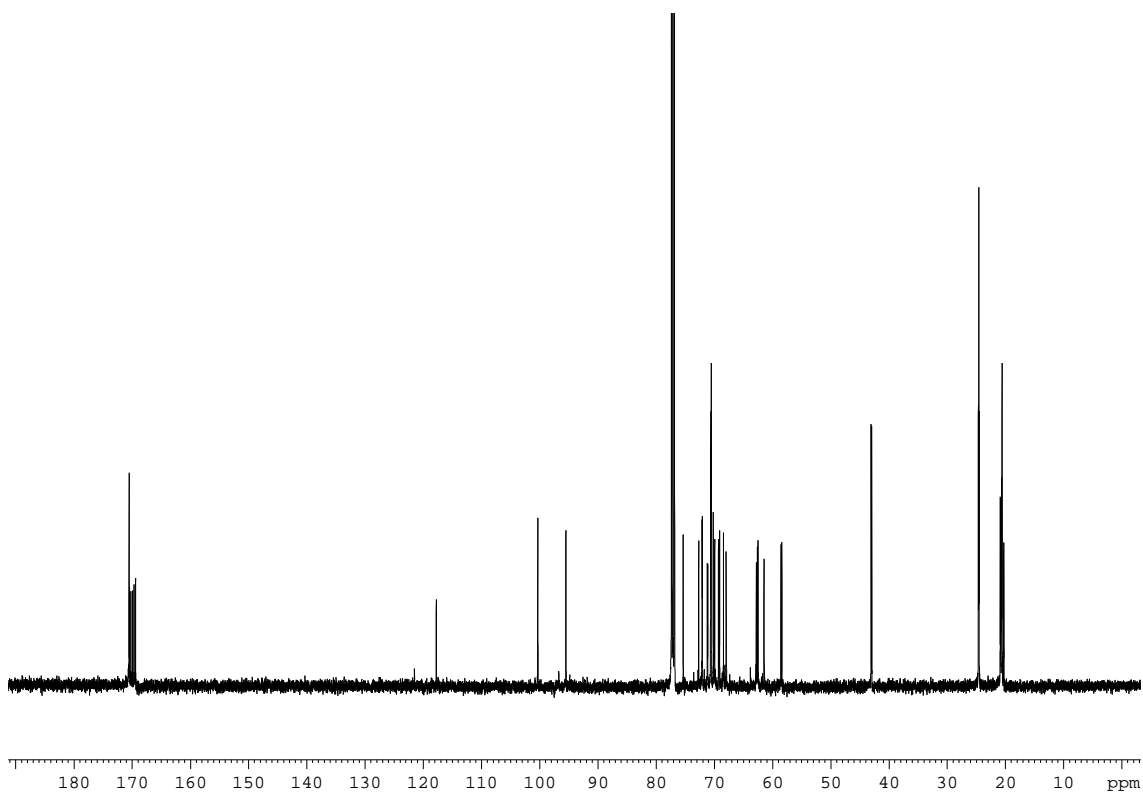
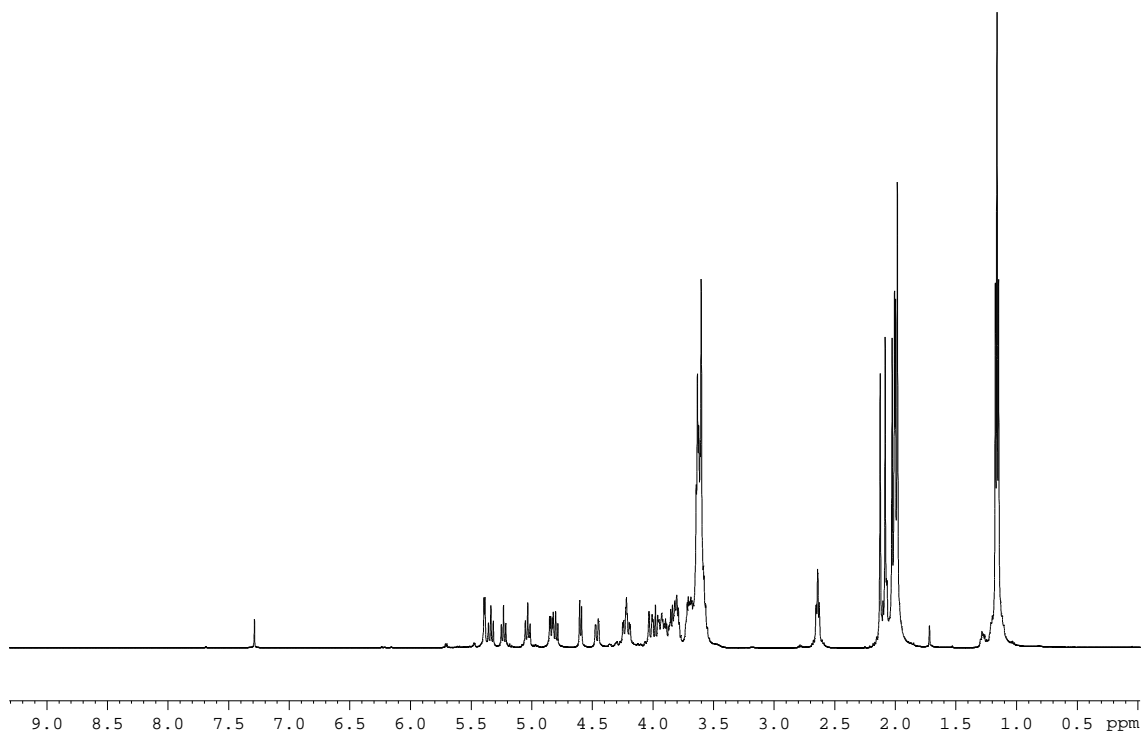
$^1\text{H-NMR}$ and $^{13}\text{C-NMR}$ spectra

Compound 18



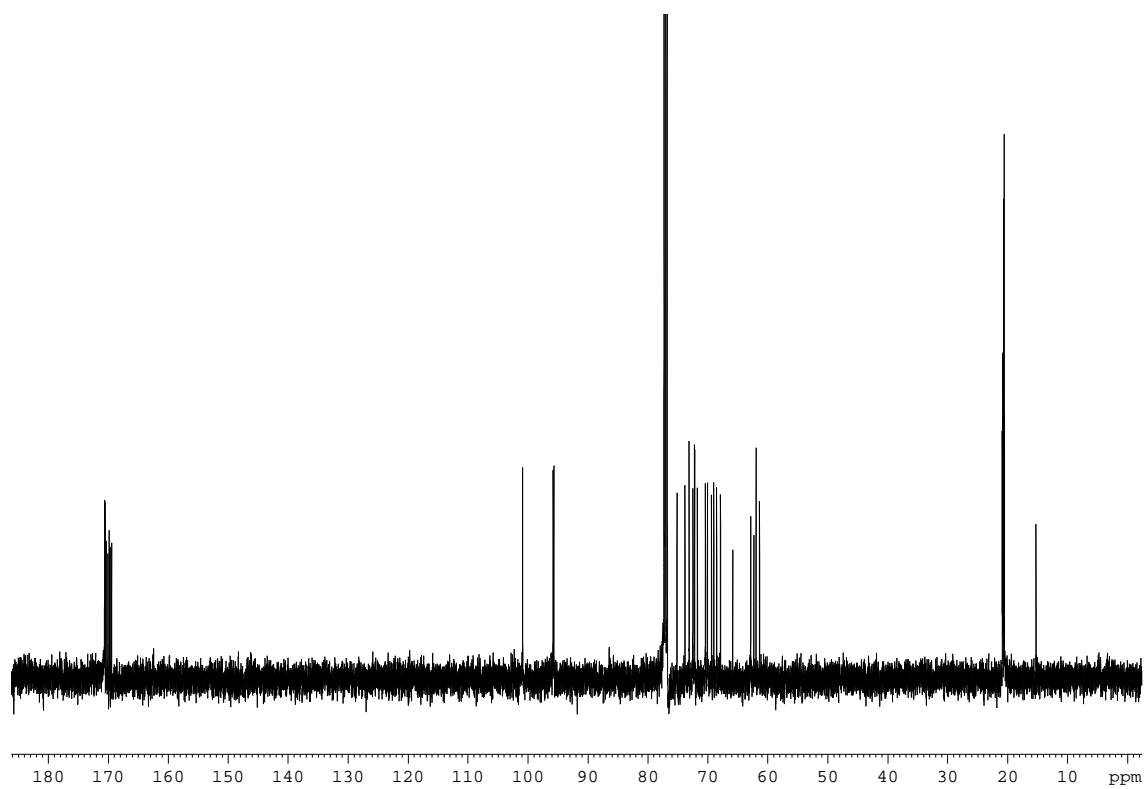
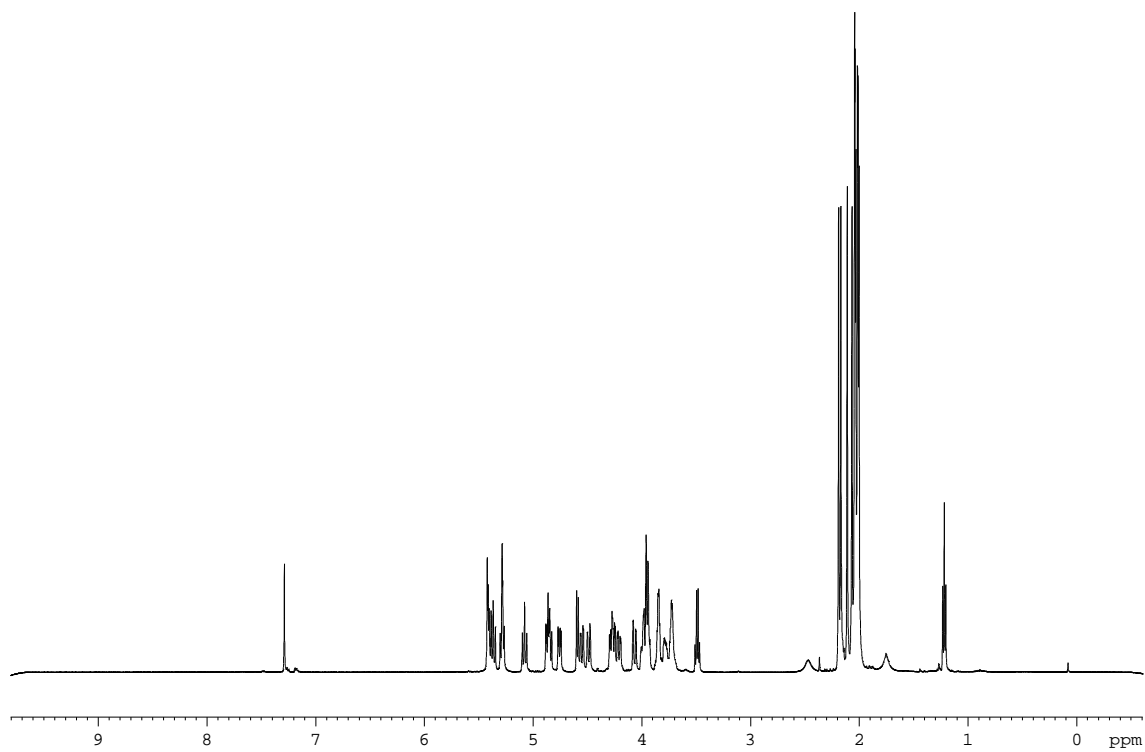
$^1\text{H-NMR}$ and $^{13}\text{C-NMR}$ spectra

Compound 19



$^1\text{H-NMR}$ and $^{13}\text{C-NMR}$ spectra

Compound 21



^1H -NMR and ^{13}C -NMR spectra

Compound 22

